

Published in final edited form as:

Physiol Behav. 2009 April 20; 97(1): 76–86. doi:10.1016/j.physbeh.2009.02.003.

Mice lacking brain-type creatine kinase activity show defective thermoregulation

Femke Streijger^{a,d}, Helma Pluk^a, Frank Oerlemans^a, Gaby Beckers^a, Antonio C. Bianco^b, Miriam O. Ribeiro^c, Bé Wieringa^a, and Catharina E.E.M. Van der Zee^{a,*}

^a Department of Cell Biology, NCMLS, Radboud University Nijmegen Medical Centre, Nijmegen, The Netherlands ^b Division of Endocrinology, Diabetes and Hypertension, Brigham and Women's Hospital, Boston, Massachusetts, USA ^c Department of Biology, CCBS, Mackenzie Presbyterian University, São Paulo, Brazil ^d ICORD, Department of Zoology, University of British Columbia, Vancouver, B.C., Canada

Abstract

The cytosolic brain-type creatine kinase and mitochondrial ubiquitous creatine kinase (CK-B and UbCKmit) are expressed during the prepubescent and adult period of mammalian life. These creatine kinase (CK) isoforms are present in neural cell types throughout the central and peripheral nervous system and in smooth muscle containing tissues, where they have an important role in cellular energy homeostasis. Here, we report on the coupling of CK activity to body temperature rhythm and adaptive thermoregulation in mice. With both brain-type CK isoforms being absent, the body temperature reproducibly drops ~1.0°C below normal during every morning (inactive) period in the daily cycle. Facultative non-shivering thermogenesis is also impaired, since CK^{−/−} mice develop severe hypothermia during 24 h cold exposure. A relationship with fat metabolism was suggested because comparison of CK^{−/−} mice with wildtype controls revealed decreased weight gain associated with less white and brown fat accumulation and smaller brown adipocytes. Also, circulating levels of glucose, triglycerides and leptin are reduced. Extensive physiological testing and uncoupling protein1 analysis showed, however, that the thermogenic problems are not due to abnormal responsiveness of brown adipocytes, since noradrenaline infusion produced a normal increase of body temperature. Moreover, we demonstrate that the cyclic drop in morning temperature is also not related to altered rhythmicity with reduced locomotion, diminished food intake or increased torpor sensitivity. Although several integral functions appear altered when CK is absent in the brain, combined findings point into the direction of inefficient neuronal transmission as the dominant factor in the thermoregulatory defect.

Keywords

Creatine kinase; Creatine kinase double knockout mice; White adipose tissue; Brown adipose tissue; Thermogenic activity; UCP1 mRNA

1. Introduction

In tissues like muscle and brain, the often high and fluctuating ATP demands require strict maintenance of energy homeostasis with tight coupling between energy production and

*Corresponding author: Dept of Cell Biology, NCMLS, Radboud University Nijmegen Medical Centre, P.O. Box 9101, 6500 HB Nijmegen, The Netherlands. Tel.: +31 24 361 4296; fax: +31 24 361 5317. streijger@icord.org (F. Streijger), i.vanderzee@ncmls.ru.nl (C.E.E.M. Van der Zee).

consumption. One of the enzymes that play a key role in the buffering and fast transfer of cellular fuel in a wide variety of tissues is creatine kinase [1–8]. Creatine kinase (CK) isoenzymes catalyse the synthesis of phosphocreatine (PCr) and its subsequent use in the regeneration of ATP by the reaction $\text{MgATP}^{2-} + \text{Cr} \leftrightarrow \text{MgADP}^{-} + \text{PCr}^{2-} + \text{H}^{+}$. In brain, two isoforms of creatine kinase are present, each encoded by separate genes, i.e. the cytosolic brain creatine kinase (CK-B) and the mitochondrial ubiquitous creatine kinase (UbCKmit). We have shown that mice deficient for both CK-B and UbCKmit (CK^{-/-}UbCKmit^{-/-} mice) have a severely abnormal phenotype [9,10] with permanently reduced body weight, impaired spatial learning, low nestbuilding activity, impaired hearing, vestibular dysfunction, and partially abnormal morphology of the hippocampal brain structure.

Here we report on an entirely new phenotypic aspect, i.e., the observation that CK^{-/-}UbCKmit^{-/-} double knockout mice have problems with maintenance of temperature homeostasis and incidentally succumb due to a sudden and severe drop in body temperature. Responses to maintain normal body temperature are coordinated by neuroendocrine interactions and the autonomic nervous system. The control of body temperature takes place in the central nervous system at different locations and levels in the spinal cord, the lower brainstem, and hypothalamus [11–16]. Of the sites in the hypothalamus the preoptic area, paraventricular, dorsomedial and ventromedial nuclei are critical areas mediating temperature homeostasis in mammals. Outside the brain, brown adipose tissue (BAT), muscle, or the tail veins are the most important effector systems for heat loss compensation [15].

Through a series of experiments, we studied possible associations between combined CK-B/UbCKmit activity and general abnormalities in food intake, body composition, or energy metabolism and compared key aspects of thermal physiology between wildtype and CK^{-/-}UbCKmit^{-/-} mice.

2. Materials and methods

2.1. Animals

The generation of brain-type creatine kinase double knockout (CK-B^{-/-}UbCKmit^{-/-}) mice (further referred to as CK^{-/-}UbCKmit^{-/-} mice) and genotype analysis was described in detail elsewhere [10]. Male adult (3–8 months) CK^{-/-}UbCKmit^{-/-} mice and age-matched male adult wildtype mice with the same genetic background (25% 129/Ola and 75% C57BL/6) were used. As reported earlier, the body weight of adult male CK^{-/-}UbCKmit^{-/-} mice (from 22 g (3 months) to 25 g (8 months)) is significantly less than that of male wildtype mice (from 28 g (3 months) to 35 g (8 months)); [10] and this study). In some experimental set-ups we included young male wildtype animals (6 weeks old; ~22 g) to have better reference matching for the effects of lower bodyweight.

All mice were housed in the central animal facility with room temperature controlled at 21°C, and an artificial 12 h:12 h light: dark cycle (lights on at 07:00 am). The mice were housed in Macrolon type II cages with food and water available ad libitum. Each cage was supplied with a mouse igloo, which serves as environmental enrichment and provides security and a nesting area for mice (PLEXX, Elst, The Netherlands).

All procedures involving animals were approved by the Animal Care Committee of the Radboud University Nijmegen Medical Centre (RU-DEC) conform the guidelines of the Dutch Council for Animal Care and the European Communities Council Directive of 24 November 1986 (86/609/EEC).

2.2. Body temperature measurements

2.2.1. At room temperature—To minimize the influence of handling on measuring body temperature, the ELAMS animal identification and body temperature monitoring system was used (PLEXX, Elst, The Netherlands). Temperature-sensitive transponders (model IPTT-300) were subcutaneously implanted into the dorsal thorax region of adult male mice from each genotype. The body temperature of mice during the course of experiments was recorded using the wireless scanner (model DAS-5004, PLEXX, Elst, The Netherlands). Body temperatures were measured between 09:00 and 11:00 h (morning) and between 15:00 and 16:00 h (afternoon) at 12 different days in a period of 23 days, both for single-housed mice (data not shown) and for group-housed mice (data shown). For the group-housed mice we also obtained a 30-hour profile, with body temperatures recorded every 3 h; this latter experiment was repeated twice. Average body temperature in °C was calculated for each time point.

2.2.2. During cold exposure—Body temperatures were first measured in mice kept at room temperature (~21°C; 21:00 h) and then at 6 h intervals during a 24-hour cold exposure (4°C) using the implanted temperature-sensitive transponders. In the first experiment single-housed animals were followed, in the second experiment group-housed mice (2–3 per cage) were recorded. When the body temperature of a mouse dropped below 28°C, the animal was removed from the cold.

2.2.3. During fasting—Adult wildtype and CK^{-/-} mice, single-housed, were fasted for 12 h in their animal room (~21°C). Body temperatures were measured just before fasting (onset at 17:00h) and then at 5, 8, 12 h of fasting, using the implanted temperature-sensitive transponders. Finally, at 30 min after the animals were given free access to food, recovery of body temperature during arousal was recorded.

2.2.4. Following acute stress—Adult mice (wt $n=10$; CK^{-/-} $n=10$) were subjected to four different unpredictable stressors, with a 2-day interval. The stress consisted of exposure to: (a) a 4-hour stay in a tilted home cage with the bottom placed at an angle of 20°, (b) a 2-min transport from the housing room to an experimental room, (c) restraint for 20 min in a small transparent round tube (7×4×4 cm), or (d) a 2-min swim in a pool (diameter 120 cm) filled with water of ~22°C. Body temperatures were measured before transport to the test room. The animals were then left for 1 h in the test room before being exposed to either test a, c or d. Body temperatures were measured directly after exposure to the stressor.

2.3. Daily food intake

Mice were individually housed and had unrestricted access to a pre-weighted (~200 g) amount of pellets in the foodhopper. For three days, food intake was measured every 24 h (at 09:00 h) and calculated as the average amount of pellets eaten (g) per day.

2.4. Locomotor activity profile

To assess basal activity, mice were tested in activity cages (36×24×25 cm; [17]), equipped with three photoelectric cells 2 mm above the floor. Interruptions of the infrared light beams were measured and stored electronically. Experiments were performed in sound tight, diffusely illuminated boxes with water soaked food pellets in a corner. The actual activity was measured for 48 h continuously to obtain two night and day activity cycles. Average activity counts were then calculated from the second 24-hour period, in order to minimize influence of initial stress-induced activity. The activity counts of the mice were recorded

each minute and later calculated and expressed as the average total activity counts per hour and per 3 h during the entire light (inactive) and dark (active) period.

2.5. Tissue weights and femur length

Adult mice were euthanized and the following tissues were collected and weighted: Brown adipose tissue (BAT; interscapular, subscapular and cervical), white adipose tissue (WAT; inguinal, epididymal and thorax), liver, brain and (gastrocnemius) muscle. To measure the length of the femur, anesthetized adult mice were immobilized on a plate with adjustable fixation bars for their teeth and paws. An X-ray image of the femur of the right hindlimb was taken with the leg positioned at a 90° angle. The femur length was assessed as the distance (in mm) from the inferior border of the lateral epicondyle to the superior border of the femur head.

2.6. Blood collection and plasma analysis

To minimize stress response on the day of blood collection, the time from initial cage disturbance to being anesthetized was less than 30 sec for each mouse. Blood samples were taken between 12:00 and 14:00 h by means of an orbita puncture under ether anesthesia. Blood was collected into an aprotinine (3000 units/ml) EDTA (1,5 mg/ml) tube, and was centrifuged at 6000 rpm at 4°C for 3 min. Plasma was collected and stored at -20°C until use. Measurements included leptin (mouse leptin ELISA kit, Crystal Chem Inc., Chicago, IL, USA), free fatty acids (NEFA C, WAKO Chemicals USA, Richmond, VA, USA), triglycerides (triglycerides kit, Sigma Diagnostics, St. Louis, MO, USA), and glucose (Infinity glucose reagent, Sigma Diagnostics).

2.7. BAT thermal response to noradrenaline infusion

The BAT thermal response to noradrenaline (NA) was performed as previously described [18,19]. Adult mice were anaesthetized with urethan (560 mg/kg) and chloralose (38 mg/kg) injected intraperitoneally. Mice were kept on a warming pad through the course of the experiment. A polyethylene (PE-50) cannula was inserted in the left jugular vein and later was used for NA infusion. BAT temperatures (°C) were measured using a precalibrated thermistor probe secured under the interscapular BAT pad (model YSI 427; Yellow Springs Instrument Co., Yellow Springs, OH, USA). Body temperature was measured with a colonic probe (model YSI 423; Yellow Springs Instrument Co.). The probes were connected to a high-precision thermometer (YSI Precision 4000A Thermometer; Yellow Springs Instrument Co.). Body temperature and BAT temperature were monitored during a period of ~15 min to obtain a stable baseline, and then NA (2 mg/ml) infusion was started at a rate of 0.5 µl/min for 30 min. Data were plotted over time and expressed as the mean increase in BAT and body temperature (Δ BAT; Δ Body; °C).

2.8. Western blot analysis

Interscapular BAT, epididymal WAT, liver, brain and (gastrocnemius) muscle of adult mice were isolated and immediately frozen in liquid nitrogen. The tissues were homogenized in 150 mM NaCl, 1% triton X-100, 25 mM Tris pH 8.0, 2 mM EDTA and Protease Inhibitor Cocktail (Roche Diagnostics, Mannheim, Germany). Following a 20-min incubation at 4°C, the lysates were centrifuged at 15.000 rpm for 20 min at 4°C. Protein concentration in the resulting supernatant was determined using the Bradford protein assay. The lysates were stored at -80°C until use. Protein samples were separated on a 10% SDS-page gel and transferred to nitrocellulose membranes (ECL, Amersham Pharmacia Biotech BA, Piscataway AB, Uppsala, Sweden) by western blotting. The membranes were blocked with 5% non-fat dry milk in PBST (PBS, 0.1% Tween-20) for 60 min and incubated overnight with primary mono-clonal anti-CK-B 21E10 (1:1000; [20]), polyclonal anti-UbCKmit #253

(1:1000; [21]), or polyclonal anti-UCP1 (1:5000, Chemicon International, Temecula, CA, USA) antibody at 4°C. The membranes were washed 3×5 min with PBST and incubated for 60 min with secondary peroxidase-conjugated Goat anti-Rabbit (Pierce Biotechnology Inc., Rockford, IL, USA) for use with UbCKmit and UCP1 antibodies, or ImmunoPure®Protein A/G (Pierce Biotechnology Inc) for use with CK-B 21E10 antibodies. Following a 6×5 min wash with PBST, the immunoreactive bands were visualized using Lumi-Light Western Blotting Substrate (Roche Diagnostics) and exposed to autoradiography films (Kodak X-Omat, Eastman Kodak Company, Rochester, NY, USA). For the detection of brain specific creatine kinase isoforms in different tissues, an amount of 50 µg of total liver, muscle, brown and white adipose protein was loaded per lane. To prevent overexposure, the amount of total brain lysate was reduced to 10 µg. For detection of UCP1 in BAT an amount of 10 µg of total protein was loaded. To accurately quantify UCP1 on the Western blot, direct infrared fluorescence detection on the Odyssey Imaging System was used, and compared with the HSP70 signal to confirm equal protein loading.

2.9. Northern blot analysis

Interscapular BAT of naïve and 12-hour cold exposed wildtype and CK^{-/-} mice was isolated for Northern blot analyses and immediately frozen in liquid nitrogen. RNA of brown adipose tissue was isolated by the LiCl-Urea method. An amount of 3 µg of RNA was loaded on a 1% MOPS formaldehyde agarose gel. After overnight electrophoresis in MOPS buffer (20 mM MOPS pH 7.0, 0.5 mM sodium acetate, 1 mM EDTA), the RNA was transferred to a nylon membrane (Hybond-N, Amersham Pharmacia Biotech BA, Uppsala, Sweden) in 10xSSC (3 M NaCl, 0.3 M NaCitrate) overnight, and cross-linked by UV irradiation. The membranes were prehybridized for at least 1 h in (pre)hybridization buffer (250 mM Na₂HPO₄ pH 7.2, 7% SDS, 1 mM EDTA) at 65°C. Purified cDNA probes (ESTs) were labeled with α-³²P-dCTP by random hexamer priming. After removing non-incorporated radio-labeled nucleotides on Sephadex-G50 columns the probe was used for hybridization, performed overnight at 65°C. Then, blots were washed with 25 mM Na₂HPO₄ pH 7.2, 0.1% SDS, 1 mM EDTA and exposed to autoradiography films (Kodak BioMax XAR films, Eastman Kodak Company, Rochester, NY, USA). To accurately quantify UCP1 and GAPDH signals on the Northern blot, a PhosphorImager system was used. Detailed information on the ESTs and origin of the UCP1 or GAPDH cDNAs is available as “EST and gene sequences placed on the array” at www.ncmls.eu/celbio/data.htm [22].

2.10. Immunostaining for CK-B and UbCKmit

Mice were transcardially perfused with 4% paraformaldehyde in phosphate buffered saline (0.1 M PBS). Brain and interscapular BAT were dissected and postfixed for 12–15 h at 4°C. Tissues were embedded in paraffin and 6 µm sections were cut and placed on microscope slides (Superfrost/Plus glass slides, Menzel-Gläser, Germany). Sections were incubated in 0.375% H₂O₂ and 0.1% Sodium Azide for 30 min at 37°C to inactivate endogenous peroxidase, rinsed in 0.01% PBS-Tween, and incubated for 30 min in blocking buffer containing 1% BSA and 2% normal donkey serum. Sections were incubated overnight at 4°C with polyclonal rabbit primary antibody for either CK-B (1:1000; [20]), or UbCKmit (1:1000; [21]). Next, sections were incubated for 1 h with a secondary biotinylated donkey anti-rabbit antibody (1:250 in PBS-T; Vector Laboratories, USA), and for 1 h with Avidine Biotinylated enzyme Complex (Vectastain Elite ABC kit, Vector Laboratories). Then, peroxidase activity was detected with 0.04% DAB; 0.015% H₂O₂ and 0.025% nickel-ammonium-sulphate in 0.1 M Tris pH 7.6 for a maximum of 10 min. Sections were counterstained with haematoxylin for 3 min, dehydrated with ethanol and xylene and embedded in Eukitt (Electron Microscopy Sciences, Fort Washington, PA, USA) for light microscopy.

2.11. LM and EM histological analysis of brown adipose tissue

For the quantification of the brown adipocyte size, paraffin-embedded sections of interscapular BAT of adult wildtype and CK^{-/-} mice were examined histologically by means of hematoxylin-eosin staining. Three 500 μm distanced microscope slides each with four sections were used. Cells were photographed (40 \times objective) using a Nikon Coolpix 990 digital camera attached to the microscope. Fat cells from the digital images (150–200 cells per animal) were analysed with PC-image software to obtain the average brown adipocyte area (μm^2), perimeter (μm) and diameter (μm).

For transmission electron microscopy, mice were transcardially perfused with 2% glutaraldehyde and 2% paraformaldehyde in 0.1 M sodium cacodylate buffer (pH 7.4). Interscapular BAT was removed and cut into $\sim 1\text{ mm}^3$ thick pieces. The tissues were washed three times with 0.1 M sodium cacodylate buffer over a 48-hour period, and postfixed with 1% osmium tetroxide and 1% sodium ferrocyanide in 0.1 M cacodylate buffer (3 h). After further washing (2 \times) with sodium cacodylate buffer for 3 h, the sections were dehydrated through a series of graded ethanols to propylene oxide, and embedded in Agar 100 epoxy resin (Agar Scientific Ltd. Essex, UK). Thin (100-nm) sections were cut with a diamond knife (Element Six, Cuijk, The Netherlands) on a Leica UCT ultramicrotome (Leica Microsystems GmbH, Wetzlar, Germany) and placed on 75-mesh carbon coated copper grids (Stork Veco bv Eerbeek, The Netherlands). Sections were contrasted with uranyl acetate and lead citrate and micrographs were taken with a JEOL 1010 electron microscope (Jeol Ltd., Tokyo, Japan). For each animal, 4–7 randomly taken BAT micrographs were analyzed at a magnification of 5000 \times . Per genotype (wt: $n=2$, 9 micrographs analyzed; CK^{-/-}: $n=3$, 18 micrographs analyzed) the average mitochondrial area (μm^2) and density (number of mitochondria per 10 μm^2 of cytoplasm) was estimated using manual grid point counting.

2.12. Statistics

All data are presented as means \pm SEM. The statistical significance of differences between two groups was assessed using the independent Student's *t*-test. Differences in body temperature within a group were analyzed using the paired *t*-test. For experiments with three groups (age- and weight-matched wildtype and CK^{-/-} mice), a one-way ANOVA followed by Bonferroni's post-hoc test was performed. To analyze group differences over time the ANOVA repeated measures was applied. All statistical procedures were performed using the SPSS software package. Statistical significance was set at $P<0.05$.

3. Results

Continuous observation over several generations of single-housed and group-housed mice that belonged to a large breeding cohort of CK^{-/-} mice revealed that individual animals ($\sim 2\%$ of the cohort) incidentally succumbed due to a sudden and severe drop in body temperature. These animals appeared to have a body temperature lower than 31 $^{\circ}\text{C}$, and most of them could be rescued by placement under a heating lamp. In order to advance our understanding of the cause of these problems we started a systematic analysis of various physiological parameters in CK^{-/-} mice, and made a comparison with the situation in wildtype animals.

3.1. CK^{-/-} mice have a lower morning body temperature

The average body temperature profiles for both wildtype ($n=20$) and CK^{-/-} ($n=18$) mice showed a correlation with the inactive (light phase) and active (dark phase) period (Fig. 1). Wildtype mice, housed at room temperature, showed average body temperatures alternating between $36.7\pm 0.1^{\circ}\text{C}$ and $37.3\pm 0.1^{\circ}\text{C}$ during the light and dark period,

respectively. Throughout the three successive 30 hour periods of recording, the average body temperature of CK^{-/-} mice during the early dark phase was similar to that of wildtypes. Later in the dark phase the body temperature of CK^{-/-} mice started to decrease and remained abnormally low during a period of 6 h. One hour before light-onset, CK^{-/-} body temperature was $\sim 0.5^{\circ}\text{C}$ lower than in wildtypes (wt: $37.2 \pm 0.1^{\circ}\text{C}$; CK^{-/-}: $36.7 \pm 0.1^{\circ}\text{C}$; $P < 0.007$; Fig. 1), and dropped further to a $\sim 1^{\circ}\text{C}$ difference at 09:00 am, which was 2 h after the start of the light period (wt: $36.9 \pm 0.1^{\circ}\text{C}$; CK^{-/-}: $35.9 \pm 0.2^{\circ}\text{C}$; $P < 0.001$; Fig. 1). During the second half of the light period the average body temperature in CK^{-/-} mice slowly increased and was no longer significantly different from wildtypes thereafter. The consistency of these observations was confirmed by repeated recordings within a time interval early in the light period (light onset 07:00 am, measurements in 09:00–11:00 am period) at 12 different days during a period of 23 days. The average morning body temperature was $36.7 \pm 0.1^{\circ}\text{C}$ for wildtypes and $35.6 \pm 0.2^{\circ}\text{C}$ for CK^{-/-} mice ($n=10$ per genotype; $P < 0.001$).

3.2. CK^{-/-} mice are unable to sustain body temperature during cold exposure

Next, to investigate the adaptive responses of CK^{-/-} mice ($n=12$) and wildtypes ($n=10$) to cold exposure, we transferred animals to a 4°C environment and measured their body temperature after 6, 12, 18 and 24 h, which included a light and dark period (Fig 2). At the start of the experiment, 2 h after onset of the dark period, the body temperature of both genotype groups did not differ (wt: $37.4 \pm 0.2^{\circ}\text{C}$; CK^{-/-}: $37.6 \pm 0.2^{\circ}\text{C}$; Fig. 2). During cold exposure, wildtype mice acclimatized well and maintained body temperature at $36.7 \pm 0.1^{\circ}\text{C}$, only 0.7°C below normal during the entire 24-hour cold period (Fig. 2). CK^{-/-} mice displayed significant reductions in body temperature. Within 18 h after onset of the experiment, all CK^{-/-} mice showed severe hypothermia and 33% (4 out of 12; not included further in the analysis) died when their body temperature dropped below 28°C . The remaining CK^{-/-} mice showed a persistent $3\text{--}5^{\circ}\text{C}$ body temperature drop ($F(1,16)=38.658$, $P < 0.001$; Fig. 2) during the exposure to cold. Post hoc testing revealed that their body temperature declined significantly already after the first 6 h following cold exposure and remained consistently low further (6 h: $P < 0.001$; 12 h: $P < 0.001$; 18 h: $P < 0.007$; 24 h: $P < 0.009$; Fig. 2).

Because CK^{-/-} mice are significantly smaller (~ 23 g) compared to age-matched wildtype mice (~ 31 g; [10]) we assessed confounding effects of reduced body size in a cohort of weight-matched young wildtype animals (6 weeks old; ~ 22 g; $n=11$). In these young animals we observed a slight drop of approximately 0.5°C in body temperature, but no further decrease occurred during the entire 24-hour cold exposure period. Taken together, the results suggest that genotype and not body size or weight is the determining factor in the effects observed.

3.3. Light and dark period rhythm of locomotor activity in CK^{-/-} mice

Increased skeletal muscle activity tends to increase body temperature by accelerating fuel oxidation [23]. Hence, the temperature profile typically parallels the profile of physical activity. To investigate whether alterations in this physiological circuit could explain our findings, CK^{-/-} and control mice were tested in an activity cage. As shown in Table 1, the shape of the day and night rhythm activity profile for CK^{-/-} mice was similar to that for wildtypes, with locomotor activity slowly decreasing after light onset and increasing just after the beginning of the dark phase.

Wildtype mice showed activity levels alternating between ~ 1100 counts during the day and ~ 2200 counts during the night period (Table 1). Activity of CK^{-/-} mice appeared increased by an average of 38% during the light (~ 1600 counts) and night phase (~ 3000

counts), compared to the wildtypes, but this difference did not reach significance (Table 1). Since the activity is higher, not lower, than in wildtype animals, we cannot explain the significantly lower morning body temperature in the CK^{-/-} mice as an effect of diminished locomotor activity.

3.4. CK^{-/-} mice consume less food

Thermoregulation is an adaptation of the basal metabolic rate, which in turn is related to food intake [23]. We therefore examined whether a change in food consumption could form a link to abnormal body temperature regulation in our CK^{-/-} mice. Analysis of food intake over a 3×24 h period revealed group differences for the absolute and relative food consumption (Table 1). Wildtype animals consumed 5.3±0.1 g of food per day, mainly eaten during the night, whereas food intake of CK^{-/-} mice was 17% lower. However, because CK^{-/-} mice were leaner than wildtypes (Table 1; see also [10]), the food intake expressed per gram of body weight actually exceeded that of wildtypes by 16% (Table 1). Of note, young wildtype mice in the same weight class (~22 g) consumed similar amounts of food (4.5±0.1 g per day; n=7) as CK^{-/-} mice. These data strongly suggest that thermogenic problems in the CK^{-/-} mice are not related to an abnormal food-intake balance.

3.5. Reduced serum lipid, leptin and glucose content in CK^{-/-} mice

The carbohydrate and lipid fuels for brown adipose tissue (BAT) controlled thermogenesis are glucose, triglycerides and free fatty acids [24–27], substrates which may be used either directly or stored for later use. Leptin levels in serum usually adequately reflect (among other items) the status of the energy reserves of the animal. To reveal abnormal energy regulation we compared serum levels of fuel metabolites as well as leptin between wildtype and CK^{-/-} mice (Table 1). In CK^{-/-} mice a significant reduction in serum triglycerides levels of ~39% was observed, whereas plasma glucose was down by 15% (Table 1). Although FFAs levels also appeared lower, this was not significant. The serum leptin concentration levels were found to be decreased in CK^{-/-} mice (Table 1).

3.6. CK^{-/-} mice show a similar fasting-induced body temperature response

CK enzymes play an essential role in cellular energy metabolism, and thermoregulation is closely tied to availability of fuel from carbohydrate or lipid intake. During periods of inefficient energy supply, mammals lower their body temperature and metabolic rate to conserve fuel [16,28–34]. To investigate if CK deficiency has resulted in a negative energy balance at the whole body level, we analyzed whether CK^{-/-} mice were more sensitive to an overnight fast. Using temperature-sensitive transponders, the body temperature response was monitored prior to and following 12-hour fasting in CK^{-/-} mice and wildtypes (n=10 per group; Fig. 3A–B). In response to the fasting, both genotype groups showed an equal drop of 4–5°C in body temperature evident late in the dark phase, with wildtype and CK^{-/-} mice having average body temperatures of 33.8±0.9°C (Fig. 3A) and 32.2±1.0°C, respectively (Fig. 3B). When food restriction was terminated by giving the animals free access to food, the fall in body temperature in wildtype and CK^{-/-} mice rapidly normalized back to initial values within 30 min (Fig. 3A–B).

3.7. CK^{-/-} mice have reduced adiposity and organ size

Next, we assessed weights of white adipose tissue (WAT, Fig. 4A) and brown adipose tissue (BAT, Fig. 4B) in wildtype (n=10–11) and CK^{-/-} (n=9–10) mice. In wildtype mice, WAT was located predominantly intra-abdominally around the epididymis, and in smaller amounts subcutaneously as thorax and inguinal white fat pads (Fig. 4A). The CK^{-/-}

mice contained a WAT mass which was reduced 40 to 50% in size, apparent in all three white fat depots (epididymal, $P<0.001$; thorax, $P<0.006$; inguinal, $P<0.003$; Fig. 4A).

Compared to wildtypes, CK^{-/-} mice have smaller cervical ($P<0.04$), subscapular ($P<0.001$) and interscapular ($P<0.003$) BAT depots as well (Fig. 4B).

Measurements of various other organs including muscle ($n=5$ both groups), brain and liver (both $n=10-11$) also showed decreased weights for CK^{-/-} mice. Muscle ($P<0.001$), brain ($P<0.02$) and liver ($P<0.001$) were 5–30% smaller (Fig. 4C). The length of the femur (CK^{-/-}, $n=5$ compared to wt, $n=12$) was chosen as an index of body size and demonstrated a reduction of 30% ($P<0.001$; Fig. 4C).

Because CK^{-/-} mice are smaller than the wildtypes we have adjusted the tissue weights data, presented in Fig. 4, also for body weight of the animals. The white and brown adipose tissues and additional organs are expressed as mg/g body weight in Table 2. Strikingly, a 7% reduction of combined BAT and a 24% reduction of combined WAT was still apparent in CK^{-/-} mice.

3.8. CK^{-/-} mice have smaller brown adipocytes

Brown adipose tissue is responsible for a major portion of thermogenesis during cold exposure in rodents [23,35,36]. To investigate if brain-type CK deficiency is associated with morphological changes in brown fat, we examined the histological appearance of BAT using light microscopy (Fig. 5A, B; $n=3$ per group) and transmission electron microscopy (Fig. 5C, D).

Brown adipocytes of adult wildtype mice (Fig. 5A) have a diameter of $25.0\pm 0.9\ \mu\text{m}$ with an area of $331\pm 9\ \mu\text{m}^2$ and in young wildtype mice a diameter of $25.7\pm 0.8\ \mu\text{m}$ with an area of $335\pm 24\ \mu\text{m}^2$. The brown adipocytes displayed their typical morphological characteristics, i.e. multilocular with the bulk of the cell body being occupied by numerous round-shaped lipid droplets (Fig. 5A, inset). At the ultrastructural level, wildtype brown adipocytes showed the characteristic high content of large mitochondria packed with cristae (Fig. 5C). In BAT of CK^{-/-} mice the typical multilocular morphology appeared to be preserved (Fig. 5B, inset). Also, no differences in mitochondrial appearance, area (wt: $0.55\pm 0.02\ \mu\text{m}^2$; CK^{-/-}: $0.61\pm 0.03\ \mu\text{m}^2$), or density (wt: 8 ± 0.6 mitochondria/ $10\ \mu\text{m}^2$ cytoplasm; CK^{-/-}: 9 ± 0.4 mitochondria/ $10\ \mu\text{m}^2$ cytoplasm) were observed (Fig. 5C, D). In contrast, there are significant changes in brown adipocyte cell size. The diameter is reduced (13%; $21.8\pm 0.2\ \mu\text{m}$) and the area is 24% smaller ($246\pm 4\ \mu\text{m}^2$) in CK^{-/-} mice compared to the wildtype ($P<0.02$; see insets Fig. 5A, B) or young wildtype ($P<0.02$) brown adipocytes. At this point we do not know whether this size difference is a manifestation of change in whole body energy metabolism, or reflects adaptation to another thermogenic activation profile in our CK^{-/-} model.

3.9. Noradrenaline infusion elicits normal BAT thermogenesis in CK^{-/-} mice

To determine whether creatine kinase deficiency causes abnormalities in BAT functioning, we investigated the ability of CK^{-/-} mice to mount a nonshivering thermogenic response. An additional group of animals was measured for noradrenaline-stimulated heat production (according to [18,19]) in interscapular BAT (Fig. 6A; wt, $n=9$; CK^{-/-}, $n=6$). At the start of the experiment, the BAT temperature of both groups did not differ (wt: $35.6\pm 0.3^\circ\text{C}$; CK^{-/-}: $36.2\pm 0.2^\circ\text{C}$). Within 30 min, noradrenaline infusion elicited a rapid and progressive increase of 2.5 to 3°C in BAT temperature in both cohorts (wt: $2.91\pm 0.21^\circ\text{C}$; CK^{-/-}: $2.50\pm 0.94^\circ\text{C}$). Thus, in spite of the size differences, brown adipocytes in CK^{-/-} and wt differ not overtly in their ability to mount a thermogenic response. Notably, BAT temperatures were measured using a precalibrated thermistor probe secured

under the interscapular BAT pad and body temperature was determined with a probe placed into the rectum. Consistently, the temperature increment was higher in BAT (Fig. 6A) than in rectum (Fig. 6B), indicating that BAT warming in either genotype group was not due to indirect heating by the body. These observations suggest that BAT in CK^{-/-} mice can respond normally to sympathetic noradrenaline activation.

3.10. Other stress-induced thermogenesis effects

The apparent intactness of stress-signaling connections to thermogenesis in CK^{-/-} mice was confirmed in other tests, where animals were exposed to different acute stressors. As listed in Table 3, cage transportation caused a stress-induced body temperature rise of 1–1.5°C in both wildtype and CK^{-/-} knockout mice. Similarly, a rise in temperature of 1–1.5°C was observed when animals were subjected to a 20 min-restraint stress. A decrease of 4.5°C in body temperature was observed in both groups following a 2-min swim in water of ~22°C, whereas the tilted cage condition did not result in a temperature change (Table 3). Thus, both genotype groups respond similarly to the four different stressors.

3.11. CK^{-/-} mice show similar UCP1 mRNA in BAT after cold exposure

The primary molecule involved in thermogenesis is uncoupling protein-1 (UCP1), located in the inner membrane of mitochondria of brown adipocytes [23,37]. Noradrenaline released from sympathetic nerve endings to BAT is the primary regulator of UCP1 activity and expression. β -Adrenergic-receptor stimulation increases UCP1 activity within seconds of stimulation, while chronic stimulation over hours and days results in increased amounts of UCP-1 protein [38]. To examine whether CK^{-/-} mice use the sympathetic outflow to BAT adequately, we used the induction of UCP1 as an indicator (Fig. 7) and measured UCP1 mRNA and protein levels in dissected interscapular BAT, before and after 12 h cold exposure ($n=3$ per genotype group/condition).

Basal UCP1 mRNA levels were not significantly different in wild-type and CK^{-/-} mice when the animals were kept at room temperature (Fig. 7A). Cold exposure for 12 h at 4°C significantly increased UCP1 mRNA expression in brown adipose tissue of wildtype animals (~200%) and in that of CK^{-/-} mice (~300%; Fig. 7A). In both genotype groups, the levels of UCP1 protein had not changed and appeared similar before and after cold exposure (Fig. 7B–E). Since no protein induction was seen, the period of cold exposure used may have been too brief to elicit an effect at the level of UCP1 protein translation (Fig. 7D–E).

3.12. CK expression in tissues involved in thermogenesis

Finally, we used western blot analysis ($n=3$ mice per group) and immunocytochemistry ($n=4$ mice per group) to see whether we could find overlap between cells and tissues with prominent CK-B and UbCKmit expression and known sites involved in body temperature regulation, such as specific hypothalamic areas in the brain, adipose tissue and muscle. With these analyzes we anticipated to reveal what end of the brain-fat axis is most dominantly involved in the thermogenic abnormality. As shown in Fig. 8A, CK-B and UbCKmit were highly expressed in total brain lysates of wildtype mice, whereas no expression was observed in thermoregulatory active brown adipose tissue and skeletal muscle. Only at very long exposure time, weak levels of UbCKmit could be detected in white adipose tissue (WAT) lysates. Additional immunocytochemistry of wildtype BAT (Fig. 8B) and WAT (data not shown) also revealed no CK-B and UbCKmit staining in the adipocytes. However, the nerves innervating the adipose tissue and also blood vessels stained clearly positive for CK-B (Fig. 8B). Interestingly, the CK-B expression in blood vessels was restricted to the smooth muscle layer. UbCKmit presence in adipose innervating nerves was undetectable, while in the smooth muscle cells a high degree of background staining was observed with

the UbCKmit specific antibody. Immunostaining for CK-B and UbCKmit in wildtype brain showed a strong expression throughout the brain, including regions known to be involved in the regulation of body temperature, like the arcuate nucleus (Arc), medial preoptic area (mPOA), and paraventricular nucleus (PVN) (Fig. 8C). Although our analyses did not discriminate between astrocyte- or neuronal expression here, we know from own and other studies that CK-B expression is prominent in astrocytes, and largely confined to inhibitory neurons [data not shown; [6,39]]. Our combined data strongly suggest that muscle and fat cells can be considered natural knockout cells for CK-B and UbCKmit. We therefore propose that the thermogenic defect that is caused by complete knockout of CK activity must originate at the “regulatory” neural end, rather than the “receiving” adipose end, of the brain-fat axis.

4. Discussion

The present study shows that the manifestation of problems in body temperature maintenance during the daily cycle and, more severely, upon cold challenge, is an integral element in the entire set of complex physiological changes that occur in the CK^{-/-} mice. We demonstrate that young and small wildtype mice, selected for comparable lower bodyweight and food intake, did not show the temperature drop below normal in the morning hours or when exposed to cold. Thus, thermogenic disbalance cannot be simply explained in terms of coupling with one separated phenotypic entity, such as reduced body size. Earlier, we already showed that also behavioral aspects of the CK^{-/-} phenotype are not a simple addition of characteristics of CK-B or UbCKmit single knockouts [6,10,40].

Some physiological conditions are known to alter heat production, sometimes with pathological consequences but often with advantageous effects. During food restriction, hypothermia is observed in several mammalian species to conserve energy by reducing metabolic heat production. When an animal faces energy deficiency, body temperature gradually decreases selectively during the early onset of the inactive (light) period, whereas body temperature in the active (dark) period is well maintained at the control level (for example see [31]). During fasting mice can show a controlled drop in body temperature to below 31°C, a condition known as torpor [28–30,32,33]. Freeman *et al.* [41] found an association between reduced endogenous serum leptin concentrations and (torpor-like) hypothermia. Since CK^{-/-} mice have reduced serum leptin levels, likely because of reduced white fat pads (see [42]), we explored the possibility of torpor-like hypothermia. However, CK^{-/-} mice appeared to be not more sensitive to 12 h fasting-induced torpor than wildtype mice. The morning hypothermia in CK^{-/-} mice can therefore not be simply explained as a torpor-like phenomenon.

The hypothermia at room temperature in CK^{-/-} mice was especially evident during the early light (inactive) phase of the day. Later on in the day and during the early dark period, CK^{-/-} mice are capable of maintaining their body temperature at normal level. Motor activity may contribute to normalization of heat maintenance during this phase, as locomotion analysis showed that CK^{-/-} mice tend to be more active.

Control of arteriolar blood flow regulates how much heat is lost through specialized heat exchange organs, such as the tail [31]. Over time, shivering disappears and other mechanisms become prominent like increased non-shivering thermogenesis in brown adipose tissue [23,38]. With CK protein being expressed in the smooth muscle layer of arteries, we cannot a priori exclude the possibility that creatine kinase deficiency could affect cutaneous vasomotion. Blood flow between the thermal core and the body surface is a thermoregulatory mechanism for heat transfer between the body and the environment [31,43–47]. In hypothermic animals, vasoconstriction suppresses peripheral blood flow and

slows heat transfer between the skin surface and the thermal core. However, pilot experiments did not reveal changes in blood pressure or vasoconstriction characteristics (F. Streijger, L. Brewster, unpublished observations), suggesting that defective control of arteriolar blood flow is not a major factor involved in the thermogenic phenotype of CK^{-/-} mice.

When an animal is acutely exposed to a cold environment, body temperature homeostasis is facilitated by behavioral strategies and physiological responses [13,15]. Huddling among group-housed animals can reduce the loss of body warmth [48]. There seemed to be no difference in huddling activity for the two genotype groups (unpublished observations, CEEM Van der Zee). In addition, the fact that group-housed and single-housed CK^{-/-} mice both showed a lower morning body temperature and that both housing conditions resulted in a problematic cold exposure response indicates that the defective thermoregulation is an intrinsic characteristic of the CK^{-/-} phenotype.

The CK^{-/-} mice consume less food when expressed in gram per day (but eat relatively more when expressed in mg per g body weight) and have reduced serum levels of glucose and free fatty acids. A negative energy balance at the whole body level due to creatine kinase deficiency may thus explain the inability to maintain normal body temperature during a cold challenge. We found that CK^{-/-} mice showed severe hypothermia already after 6 h cold exposure. Because cold exposure increases O₂ uptake and basal metabolic state [38], and survival in the cold depends on increased energy expenditure, a sustained substrate mobilization from the main energy stores such as liver glycogen and adipose tissue is required. A substantially diminished adiposity content (reduced WAT, BAT and brown adipocytes size) was observed in CK^{-/-} mice compared to wildtypes, limiting substrate availability for thermogenesis. However, if CK deficiency has resulted in a negative shift in energy homeostasis one would expect fasting-induced hypothermia to be more pronounced in CK^{-/-} mice, which was not the case. Our observations therefore do not support overall metabolic energy adaptation as the main cause for diminished performance in adaptive thermogenesis in CK^{-/-} mice.

So, what remains as an acceptable explanation for the observed phenotype? Based on our findings, the thermogenic defect cannot be easily explained at the level of intrinsic BAT functioning, since noradrenaline infusion successfully increased BAT and body temperature in CK^{-/-} mice. Also other stress-induced body temperature signaling appeared functional intact. Importantly, western blot analysis and immunohistochemistry of BAT indicated that the creatine kinase isoforms are not detectably expressed in brown adipocytes, but are present in nerves innervating BAT and in BAT arteries of wildtype tissue. Because we used highly specific antibodies against both CK-B and UbCKmit, the finding of others [49,50], who reported creatine kinase activity in whole adipose tissue lysates, are most likely best explained by enzymatic “contamination” from nerves and arteries in BAT tissue.

Collectively, these arguments and findings point into the direction of dysfunctional regulation of thermogenesis by the neural circuitry, with adaptational or direct involvement of CNS areas or defective signaling through PNS systems, as the most likely explanation for the CK^{-/-} body temperature problems. Afferent and efferent pathways governing the thermoeffectors involve the spinal cord, medulla oblongata, midbrain/pons, and hypothalamus [13,15,51], areas in which brain-type CK is prominently expressed and has a supportive and distributing role in glial and neural cell energetics [5,6,10,40]. Conti *et al.* [52] reported that overexpression of UCP2 in orexin/hypocretin neurons resulted in elevated hypothalamic temperatures, forcing the hypothalamus to lower body temperature 0.3–0.5°C, mostly seen in the second part of the night. This resembles closely the morning hypothermia observed in CK^{-/-} mice, indicating that a metabolic alteration in a purely neuronal and

spatially confined population of cells can be sufficient to cause a cyclic drop in body temperature.

In conclusion, our data suggest that efficient neuronal communication between different hypothalamus circuits involved in thermo-regulation is lost as a result of CK deficiency. Further study is needed to see whether loss of function elsewhere in the brain could also attribute to thermo-related problems in the complex and multi-systemic phenotype of CK^{-/-} mice. More study is also needed to precisely pinpoint the thermogenic defect to specific mechanistic effects in neuronal and/or glial cells, but in view of the widespread cell-metabolic role of CK activity [7,8] this remains a formidable future task.

Acknowledgments

This research is supported by a research grant from the Radboud University Nijmegen Medical Centre. We want to thank Huib Croes for paraffin histology and immunocytochemistry, Mietske Wijers for her contribution to the electron microscopy study, Dr. L. Brewster for the vasoconstriction pilot experiments and our colleagues in the Central Animal Facility for support and advice regarding the animal care.

References

1. Bessman SP, Carpenter CL. The creatine-creatine phosphate energy shuttle. *Annu Rev Biochem.* 1985; 54:831–62. [PubMed: 3896131]
2. Wallimann T, Wyss M, Brdiczka D, Nicolay K, Eppenberger HM. Intracellular compartmentation, structure and function of creatine kinase isoenzymes in tissues with high and fluctuating energy demands: the ‘phosphocreatine circuit’ for cellular energy homeostasis. *Biochem J.* 1992; 281(Pt 1): 21–40. [PubMed: 1731757]
3. O’Gorman E, Beutner G, Wallimann T, Brdiczka D. Differential effects of creatine depletion on the regulation of enzyme activities and on creatine-stimulated mitochondrial respiration in skeletal muscle, heart, and brain. *Biochim Biophys Acta.* 1996; 1276(2):161–70. [PubMed: 8816948]
4. Wyss M, Kaddurah-Daouk R. Creatine and creatinine metabolism. *Physiol Rev.* 2000; 80(3):1107–213. [PubMed: 10893433]
5. in ‘t Zandt HJ, Renema WK, Streijger F, Jost C, Klomp DW, Oerlemans F, et al. Cerebral creatine kinase deficiency influences metabolite levels and morphology in the mouse brain: a quantitative in vivo ¹H and ³¹P magnetic resonance study. *J Neurochem.* 2004; 90(6):1321–30. [PubMed: 15341516]
6. Jost CR, Van der Zee CE, In ‘t Zandt HJ, Oerlemans F, Verheij M, Streijger F, et al. Creatine kinase B-driven energy transfer in the brain is important for habituation and spatial learning behaviour, mossy fibre field size and determination of seizure susceptibility. *Eur J Neurosci.* 2002; 15(10): 1692–706. [PubMed: 12059977]
7. Kuiper JW, Pluk H, Oerlemans F, van Leeuwen FN, de Lange F, Franssen J, et al. Creatine kinase-mediated ATP supply fuels actin-based events in phagocytosis. *PLoS Biol.* 2008; 6(3):e51. [PubMed: 18336068]
8. Chang EJ, Ha J, Oerlemans F, Lee YJ, Lee SW, Ryu J, et al. Brain-type creatine kinase has a crucial role in osteoclast-mediated bone resorption. *Nat Med.* 2008; 14:966–72. [PubMed: 18724377]
9. Shin JB, Streijger F, Beynon A, Peters T, Gadzala L, McMillen D, et al. Hair bundles are specialized for ATP delivery via creatine kinase. *Neuron.* 2007; 53(3):371–86. [PubMed: 17270734]
10. Streijger F, Oerlemans F, Ellenbroek BA, Jost CR, Wieringa B, Van der Zee CE. Structural and behavioural consequences of double deficiency for creatine kinases BCK and UbCKmit. *Behav Brain Res.* 2005; 157(2):219–34. [PubMed: 15639173]
11. Bamshad M, Song CK, Bartness TJ. CNS origins of the sympathetic nervous system outflow to brown adipose tissue. *Am J Physiol.* 1999; 276(6 Pt 2):R1569–1578. [PubMed: 10362733]
12. Dimicco JA, Zaretsky DV. The dorsomedial hypothalamus: a new player in thermoregulation. *Am J Physiol Regul Integr Comp Physiol.* 2007; 292(1):R47–63. [PubMed: 16959861]

13. Nagashima K, Nakai S, Tanaka M, Kanosue K. Neuronal circuitries involved in thermoregulation. *Auton Neurosci*. 2000; 85(1–3):18–25. [PubMed: 11189023]
14. Oldfield BJ, Giles ME, Watson A, Anderson C, Colvill LM, McKinley MJ. The neurochemical characterisation of hypothalamic pathways projecting polysynaptically to brown adipose tissue in the rat. *Neuroscience*. 2002; 110(3):515–26. [PubMed: 11906790]
15. Romanovsky AA. Thermoregulation: some concepts have changed. Functional architecture of the thermoregulatory system. *Am J Physiol Regul Integr Comp Physiol*. 2007; 292(1):R37–46. [PubMed: 17008453]
16. Szekely M. Orexins, energy balance, temperature, sleep-wake cycle. *Am J Physiol Regul Integr Comp Physiol*. 2006; 291(3):R530–532. [PubMed: 16556904]
17. Cools AR. Mesolimbic dopamine and its control of locomotor activity in rats: differences in pharmacology and light/dark periodicity between the olfactory tubercle and the nucleus accumbens. *Psychopharmacology (Berl)*. 1986; 88(4):451–9. [PubMed: 3085132]
18. Ribeiro MO, Carvalho SD, Schultz JJ, Chiellini G, Scanlan TS, Bianco AC, et al. Thyroid hormone-sympathetic interaction and adaptive thermogenesis are thyroid hormone receptor isoform-specific. *J Clin Invest*. 2001; 108(1):97–105. [PubMed: 11435461]
19. Ribeiro MO, Lebrun FL, Christoffolete MA, Branco M, Crescenzi A, Carvalho SD, et al. Evidence of UCP1-independent regulation of norepinephrine-induced thermogenesis in brown fat. *Am J Physiol Endocrinol Metab*. 2000; 279(2):E314–322. [PubMed: 10913031]
20. de Kok YJ, Geurds MP, Siermans EA, Usmany M, Vlak JM, Wieringa B. Production of native creatine kinase B in insect cells using a baculovirus expression vector. *Mol Cell Biochem*. 1995; 143(1):59–65. [PubMed: 7776959]
21. Friedman DL, Perryman MB. Compartmentation of multiple forms of creatine kinase in the distal nephron of the rat kidney. *J Biol Chem*. 1991; 266 (33):22404–10. [PubMed: 1939264]
22. de Groof AJ, Smeets B, Groot Koerkamp MJ, Mul AN, Janssen EE, Tabak HF, et al. Changes in mRNA expression profile underlie phenotypic adaptations in creatine kinase-deficient muscles. *FEBS Lett*. 2001; 506(1):73–8. [PubMed: 11591374]
23. Cannon B, Nedergaard J. Brown adipose tissue: function and physiological significance. *Physiol Rev*. 2004; 84(1):277–359. [PubMed: 14715917]
24. Inokuma K, Ogura-Okamoto Y, Toda C, Kimura K, Yamashita H, Saito M. Uncoupling protein 1 is necessary for norepinephrine-induced glucose utilization in brown adipose tissue. *Diabetes*. 2005; 54(5):1385–91. [PubMed: 15855324]
25. Moura MA, Festuccia WT, Kawashita NH, Garofalo MA, Brito SR, Kettelhut IC, et al. Brown adipose tissue glyceroneogenesis is activated in rats exposed to cold. *Pflugers Arch*. 2005; 449(5):463–9. [PubMed: 15688247]
26. Shimizu Y, Nikami H, Saito M. Sympathetic activation of glucose utilization in brown adipose tissue in rats. *J Biochem*. 1991; 110(5):688–92. [PubMed: 1783598]
27. Wu Q, Kazantzis M, Doege H, Ortegon AM, Tsang B, Falcon A, et al. Fatty acid transport protein 1 is required for nonshivering thermogenesis in brown adipose tissue. *Diabetes*. 2006; 55(12):3229–37. [PubMed: 17130465]
28. Himms-Hagen J. Food restriction increases torpor and improves brown adipose tissue thermogenesis in ob/ob mice. *Am J Physiol*. 1985; 248(5 Pt 1):E531–539. [PubMed: 4039535]
29. Hudson, JW. Strategies in the cold: natural torpidity and thermogenesis. Wang, LCH.; Hudson, JW., editors. Academic Press; 1978. p. 67-108.
30. Hudson JW, Scott IM. Daily torpor in the laboratory mouse, *Mus. musculus* var. albino. *Physiol Zool*. 1979; 52:205–18.
31. Nagashima K, Nakai S, Matsue K, Konishi M, Tanaka M, Kanosue K. Effects of fasting on thermoregulatory processes and the daily oscillations in rats. *Am J Physiol Regul Integr Comp Physiol*. 2003; 284(6):R1486–1493. [PubMed: 12736180]
32. Overton JM, Williams TD. Behavioral and physiologic responses to caloric restriction in mice. *Physiol Behav*. 2004; 81(5):749–54. [PubMed: 15234180]
33. Swan, H. Thermoregulation and bioenergetics. Elsevier; 1974.

34. Szekely M, Petervari E, Pakai E, Hummel Z, Szelenyi Z. Acute, subacute and chronic effects of central neuropeptide Y on energy balance in rats. *Neuropeptides*. 2005; 39 (2):103–15. [PubMed: 15752544]
35. Bachman ES, Dhillon H, Zhang CY, Cinti S, Bianco AC, Kobilka BK, et al. betaAR signaling required for diet-induced thermogenesis and obesity resistance. *Science*. 2002; 297(5582):843–5. [PubMed: 12161655]
36. Thomas SA, Palmiter RD. Thermoregulatory and metabolic phenotypes of mice lacking noradrenaline and adrenaline. *Nature*. 1997; 387(6628):94–7. [PubMed: 9139828]
37. Sell H, Deshaies Y, Richard D. The brown adipocyte: update on its metabolic role. *Int J Biochem Cell Biol*. 2004; 36(11):2098–104. [PubMed: 15313455]
38. Lowell BB, Spiegelman BM. Towards a molecular understanding of adaptive thermogenesis. *Nature*. 2000; 404(6778):652–60. [PubMed: 10766252]
39. Tachikawa M, Fukaya M, Terasaki T, Ohtsuki S, Watanabe M. Distinct cellular expressions of creatine synthetic enzyme GAMT and creatine kinases uCK-Mi and CK-B suggest a novel neuronal relationship for brain energy homeostasis. *Eur J Neurosci*. 2004; 20(1):144–60. [PubMed: 15245487]
40. Streijger F, Jost CR, Oerlemans F, Ellenbroek BA, Cools AR, Wieringa B, et al. Mice lacking the UbCKmit isoform of creatine kinase reveal slower spatial learning acquisition, diminished exploration and habituation, and reduced acoustic startle reflex responses. *Mol Cell Biochem*. 2004; 256–257(1–2):305–18.
41. Freeman DA, Lewis DA, Kauffman AS, Blum RM, Dark J. Reduced leptin concentrations are permissive for display of torpor in Siberian hamsters. *Am J Physiol Regul Integr Comp Physiol*. 2004; 287(1):R97–R103. [PubMed: 15191926]
42. Patel HR, Qi Y, Hawkins EJ, Hileman SM, Elmquist JK, Imai Y, et al. Neuropeptide Y deficiency attenuates responses to fasting and high-fat diet in obesity-prone mice. *Diabetes*. 2006; 55(11):3091–8. [PubMed: 17065347]
43. Foster, DO. *Brown Adipose Tissue*. Trayhurn, P.; Nicholls, DG., editors. Edward Arnold; 1986. p. 31–51.
44. Kikuchi-Utsumi K, Gao B, Ohinata H, Hashimoto M, Yamamoto N, Kuroshima A. Enhanced gene expression of endothelial nitric oxide synthase in brown adipose tissue during cold exposure. *Am J Physiol Regul Integr Comp Physiol*. 2002; 282(2):R623–626. [PubMed: 11792674]
45. Nakayama A, Bianco AC, Zhang CY, Lowell BB, Frangioni JV. Quantitation of brown adipose tissue perfusion in transgenic mice using near-infrared fluorescence imaging. *Mol Imaging*. 2003; 2(1):37–49. [PubMed: 12926236]
46. Wang Y, Kimura K, Inokuma K, Saito M, Kontani Y, Kobayashi Y, et al. Potential contribution of vasoconstriction to suppression of heat loss and homeothermic regulation in UCP1-deficient mice. *Pflugers Arch*. 2006; 452(3):363–9. [PubMed: 16395600]
47. Young AA, Dawson NJ. Evidence for on-off control of heat dissipation from the tail of the rat. *Can J Physiol Pharmacol*. 1982; 60(3):392–8. [PubMed: 7074424]
48. Kauffman AS, Paul MJ, Butler MP, Zucker I. Huddling, locomotor, and nest-building behaviors of furred and furless Siberian hamsters. *Physiol Behav*. 2003; 79(2):247–56. [PubMed: 12834796]
49. Berlet HH, Bonsmann I, Birringer H. Occurrence of free creatine, phosphocreatine and creatine phosphokinase in adipose tissue. *Biochim Biophys Acta*. 1976; 437 (1):166–74. [PubMed: 949504]
50. Karmali A, Montague DJ, Holloway BR, Peters TJ. Comparative subcellular fractionation of control and cold-adapted rat brown and white adipose tissue with special reference to peroxisomal and mitochondrial distributions. *Cell Biochem Funct*. 1984; 2(3):155–60. [PubMed: 6478539]
51. Kanosue K, Hosono T, Zhang YH, Chen XM. Neuronal networks controlling thermoregulatory effectors. *Prog Brain Res*. 1998; 115:49–62. [PubMed: 9632929]
52. Conti B, Sanchez-Alavez M, Winsky-Sommerer R, Morale MC, Lucero J, Brownell S, et al. Transgenic mice with a reduced core body temperature have an increased life span. *Science*. 2006; 314(5800):825–8. [PubMed: 17082459]

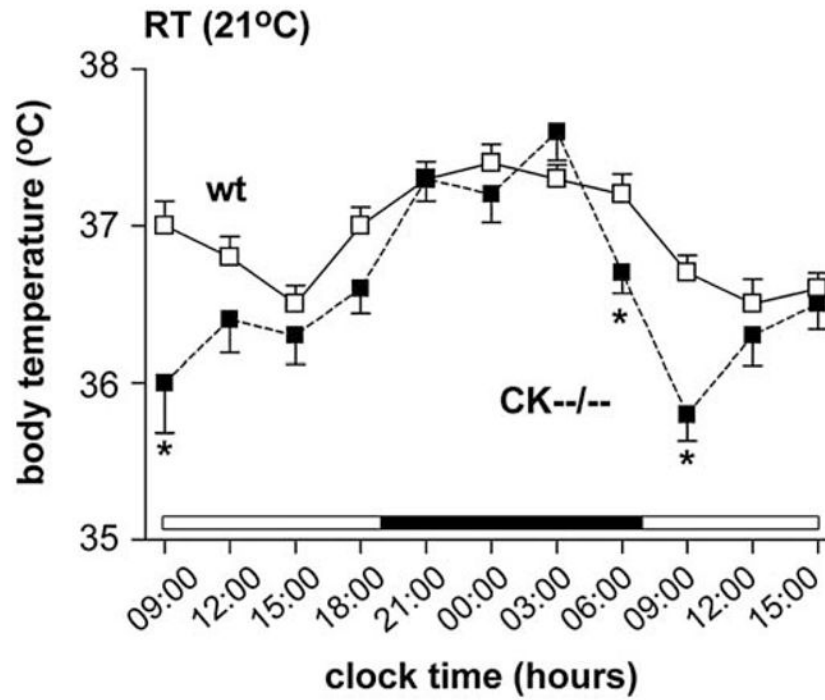


Fig. 1. Body temperature profile of wildtype and CK^{-/-} mice. At room temperature (RT) CK^{-/-} mice (black squares) demonstrated a significantly (* $P < 0.007$) lower morning body temperature compared to wildtype mice (white squares).

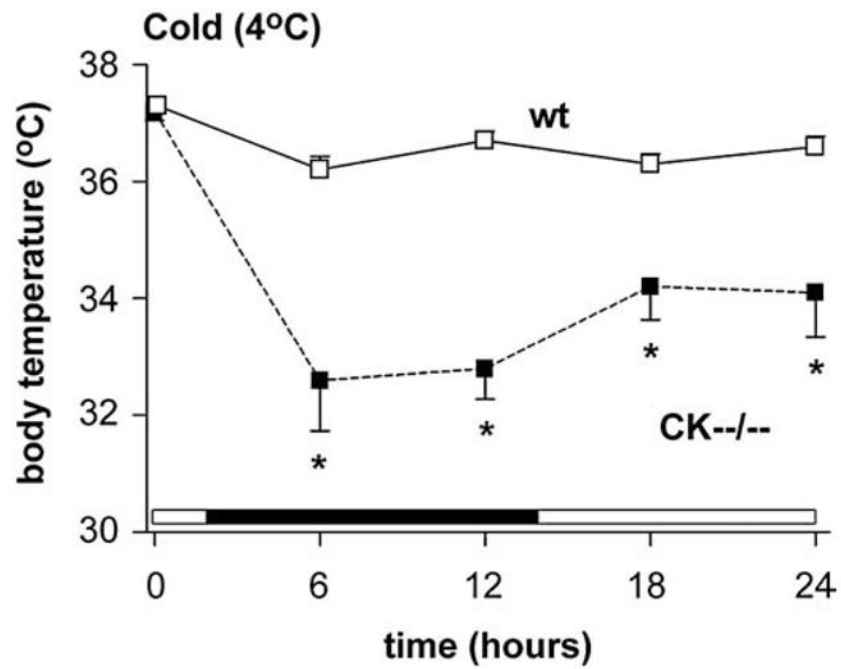
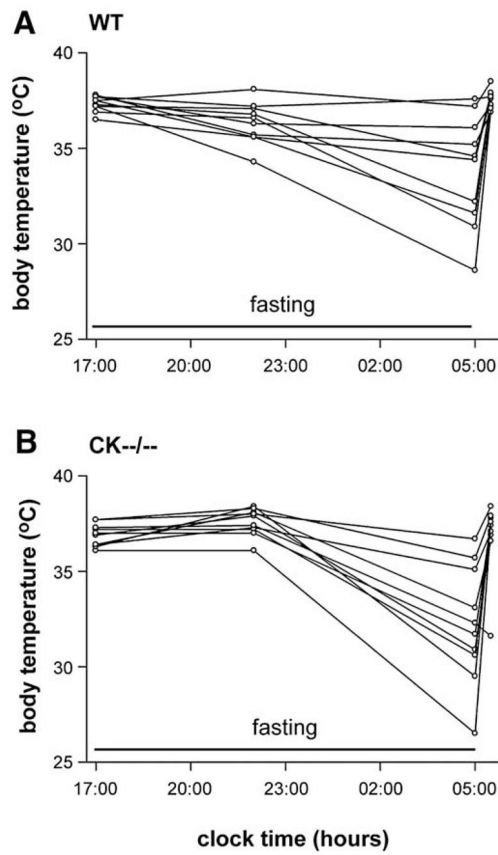


Fig. 2. Upon cold exposure, CK^{-/-} mice (black squares) were unable to sustain body temperature whereas wildtypes (white squares) could (* $P < 0.001$). Notably, 4 out of 12 CK^{-/-} mice, that died when their body temperature dropped below 28°C during the cold challenge, were not included in the analysis.

**Fig. 3.**

Fasting-induced body temperature response in wildtype and CK^{-/-} mice. In response to 12-hour fasting, an equal drop of 4–5°C in body temperature was evident late in the dark phase for (A) wildtype and (B) CK^{-/-} mice. When food restriction was terminated the fall in body temperature in both groups rapidly normalized to initial values. Lines depicted are from individual animals.

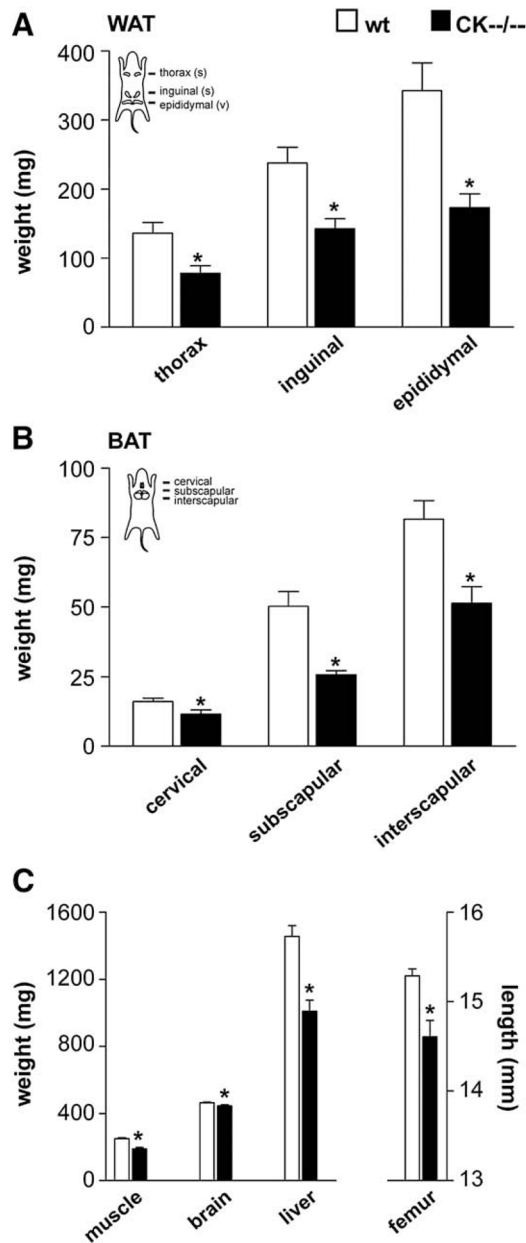


Fig. 4. Organ weight distribution of wildtype and CK^{-/-} mice. (A) CK^{-/-} mice, compared to wildtypes, show an overall decline in white adipose tissue (WAT), and (B) brown adipose tissue (BAT) mass for all three indicated fat pads. (C) Muscle, brain and liver weights, and femur length, were also smaller in CK^{-/-} mice than in wildtypes. *Significantly different from wildtype (WAT thorax, $P < 0.006$; inguinal, $P < 0.003$; epididymal, $P < 0.001$; BAT cervical, $P < 0.04$; subscapular, $P < 0.001$; inter-scapular, $P < 0.003$; muscle, $P < 0.001$; brain, $P < 0.02$; liver, $P < 0.001$; femur, $P < 0.001$).

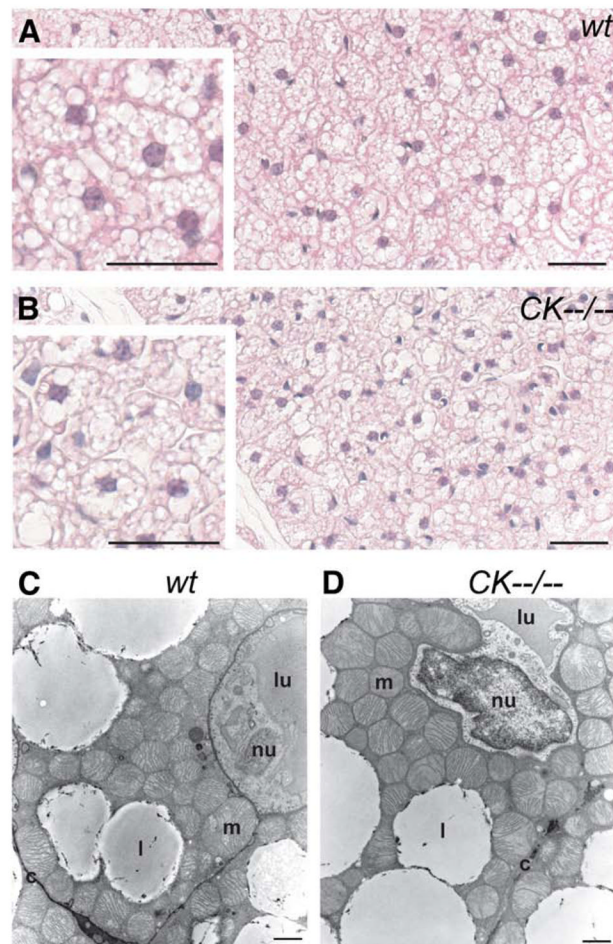


Fig. 5. Histological analysis of brown adipose tissue from wildtype and CK^{-/-} mice. (A) Both wildtype and (B) CK^{-/-} mice showed a multilocular characteristic for brown adipocytes, with the cells being occupied by numerous round-shaped fat droplets of various sizes. The inset in B, compared to the inset in A, showed a reduced adipocyte size for CK^{-/-} mice. Horizontal black bar in A, B, inset A, and inset B represents 30 μm. Electron microscopic morphometry analysis of BAT indicated no differences in mitochondrial appearance, size or density between wildtype (C) and CK^{-/-} (D) mice. Horizontal black bar represents 1 μm. l, lipid droplet; m, mitochondria; nu, nucleus; c, cell membrane; lu, capillary lumen.

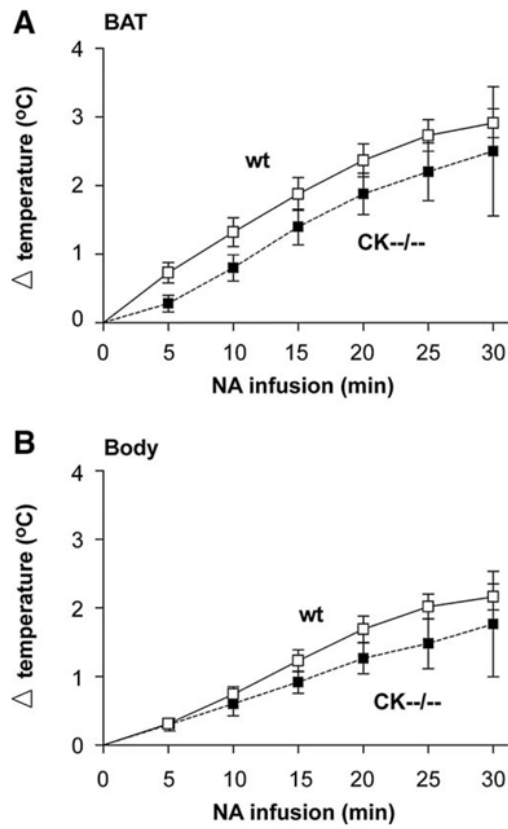


Fig. 6. Physiological temperature response to noradrenaline in wildtype and CK-/- mice. (A) noradrenaline (NA) infusion increased brown adipose tissue temperature (BAT), and (B) body temperature to a similar extent in wildtype (wt, white squares) and in CK-/- (black squares) mice.

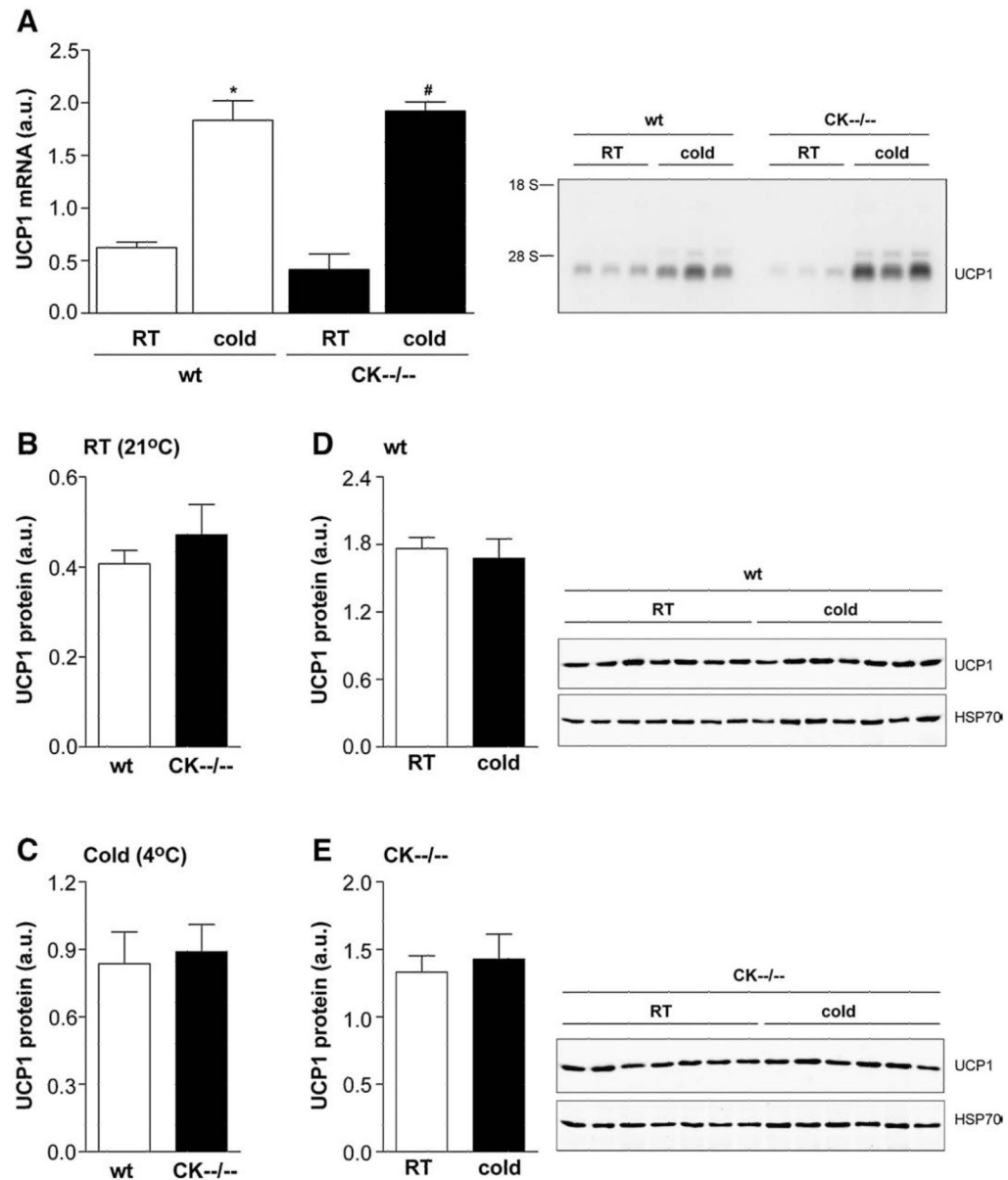


Fig. 7. UCP1 response in brown adipose tissue of cold exposed wildtype and CK^{-/-} mice shown with Northern blots (A) and Western blots (B, C, D, E). (A) UCP1 mRNA is significantly increased following 12 h cold exposure, and to the same extent, in both wildtype and CK^{-/-} mice. When compared to room temperature (RT) condition: * $P < 0.031$, # $P < 0.011$. (B) No differences were found for UCP1 protein levels under basal (RT, 21°C) and (C) cold conditions (4°C). (D–E) In both genotype groups, 12 h cold exposure did not elicit a rise in protein level.

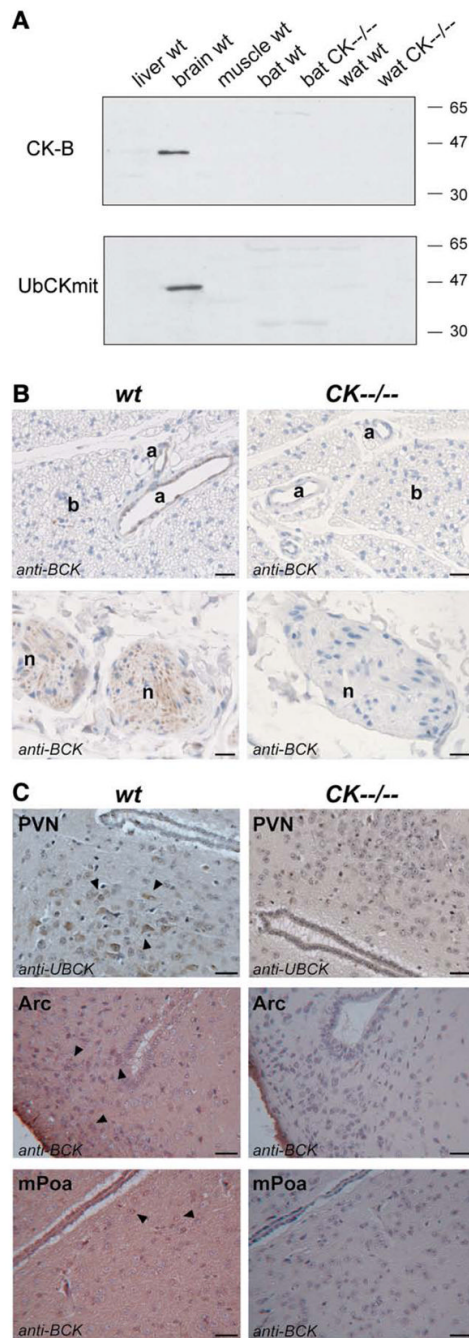


Fig. 8. Cytosolic brain creatine kinase (CK-B) and mitochondrial ubiquitous creatine kinase (UbCKmit) expression in various tissues. (A) Western blot analyses revealed immunoreactivity towards CK-B and UbCKmit in total brain lysates of wildtype (wt) animals. However, liver, muscle, brown adipose tissue (BAT) and white adipose tissue (WAT) of wildtype and CK^{-/-} mice remained negative. (B) This was consistent with the absence of immunostaining for brain-type creatine kinase (shown here: the antibody indicated as anti-BCK) in brown adipocytes (b). However, CK-B was present in arteries (a) and visible in the nerves (n) innervating BAT. Horizontal black bar represents 100 μm. (C) Immunocytochemistry performed with an antibody against brain-type creatine kinase

(indicated in Arc and mPOA pictures as anti-BCK) and an antibody against mitochondrial ubiquitous creatine kinase (indicated in PVN pictures as anti-UBCK) revealed that the CK-B and UbCKmit isoforms were expressed in brain regions that are involved in thermoregulation, like the paraventricular nucleus (PVN), arcuate nucleus (Arc) and medial preoptic area (mPOA). Horizontal black bar represents 25 μm .

Table 1Comparative behavioral and physiological analysis of wildtype and CK^{-/-} mice.

	Wildtype	CK ^{-/-}
Body weight (g)	35.1±0.7	25.4±0.8***
<i>Food intake per day</i>		
Absolute (g per animal)	5.3±0.1	4.4±0.2***
Relative (mg per animal/g bw)	151±4.9	175±6.2**
<i>Activity (counts)</i>		
Day		
06:00–09:00	409±45	613±158
09:00–12:00	250±34	365±81
12:00–15:00	242±53	392±57
15:00–18:00	247±47	280±65
Total day	1148±104	1649±263
Night		
18:00–21:00	570±192	475±61
21:00–00:00	593±99	1042±262
00:00–03:00	515±105	854±189
03:00–06:00	469±92	638±142
Total night	2247±425	3009±570
<i>Blood parameters</i>		
Glucose (mmol/l)	10.2±0.3	8.7±0.4**
Leptin (ng/ml)	1.3±0.1	0.9±0.1*
FFA (mmol/l)	0.47±0.04	0.36±0.04
TG (mmol/l)	0.60±0.08	0.37±0.04*

All values are expressed as means±SEM. bw, body weight; FFA, free fatty acids; TG, triglycerides. Number of animals $n=9-11$ per group. Significantly different from wildtype (Student's t -test):

* $P<0.05$;

** $P<0.01$;

*** $P<0.001$.

Table 2Weight of different organs (in mg/g body weight) in wildtype and CK^{-/-} mice.

	Wildtype	CK ^{-/-}
Body weight (g)	31.0±0.9	22.3±0.8**
<i>Tissues and organs (mg/g body weight)</i>		
WAT thorax	4.4±0.5	3.5±0.5
WAT inguinal	7.7±0.8	5.8±0.9*
WAT epididymal	10.3±1.2	7.8±0.9*
BAT cervical	0.4±0.1	0.5±0.1
BAT subscapular	1.5±0.2	1.2±0.1*
BAT interscapular	2.4±0.2	2.3±0.3
Muscle	7.5±0.2	8.1±0.4*
Brain	14.0±0.1	20.1±0.3**
Liver	43.9±1.9	45.5±2.9

All values are expressed as means±SEM. WAT: white adipose tissue; BAT: brown adipose tissue. Number of animals $n=9-11$ per group (except for brain, $n=5$). Significantly different from wildtype (Student's *t*-test):

* $P<0.05$;

** $P<0.001$.

Table 3

Stress-test induced changes in body temperature.

	Wildtype	CK ^{-/-}
Initial daytime body temp (°C)	36.7±0.1	35.9±0.1 [*]
<i>Stress-test (Δ°C)</i>		
Tilting cage	-0.4±0.2	-0.1±0.2
2 min-transportation	+1.1±0.1 [#]	+1.4±0.2 [#]
20 min-restraint tube	+1.1±0.2 [#]	+1.6±0.2 [#]
2 min-swimming	-4.5±0.3 [#]	-4.9±0.8 [#]

All values are expressed as means±SEM. Number of animals $n=10$ per group.

^{*} $P < 0.001$, significantly different from wildtype (one-way ANOVA),

[#] $P < 0.001$, significant decrease (-) or increase (+) in body temperature compared to their own initial daytime body temperature (paired t -test).